

# Exploring the parameter space of a rabbit ventricular action potential model to investigate the effect of variation on action potential and calcium transients

Philip Gemmell, Kevin Burrage, Blanca Rodriguez and T. Alexander Quinn

**Abstract**—Computational models for cardiomyocyte action potentials (AP) often make use of a large parameter set. This parameter set can contain some elements that are fitted to experimental data independently of any other element, some elements that are derived concurrently with other elements to match experimental data, and some elements that are derived purely from phenomenological fitting to produce the desired AP output. Furthermore, models can make use of several different data sets, not always derived for the same conditions or even the same species. It is consequently uncertain whether the parameter set for a given model is physiologically accurate. Furthermore, it is only recently that the possibility of degeneracy in parameter values in producing a given simulation output has started to be addressed. In this study, we examine the effects of varying two parameters (the L-type calcium current ( $I_{CaL}$ ) and the delayed rectifier potassium current ( $I_{Ks}$ )) in a computational model of a rabbit ventricular cardiomyocyte AP on both the membrane potential ( $V_m$ ) and calcium ( $Ca^{2+}$ ) transient. It will subsequently be determined if there is degeneracy in this model to these parameter values, which will have important implications on the stability of these models to cell-to-cell parameter variation, and also whether the current methodology for generating parameter values is flawed. The accuracy of AP duration (APD) as an indicator of AP shape will also be assessed.

## I. INTRODUCTION

In recent years, many models have been proposed and used to investigate properties of cardiomyocytes [1], [2], [3], [4], [5]. However, it is often the case that the available experimental data are insufficient to determine some parameters of the model independently, with some parameters having to be fitted on a purely phenomenological basis to produce the desired output. All too often, the caveat of some parameters being less rigorously determined than others is not emphasised, and all parameters used are given the same credence. The possible ramifications of this fitting approach, and the possibility of degeneracy of parameters—multiple different sets of input parameters giving identical measured outputs—have only recently begun to be examined.

It is the purpose of the present study to evaluate the Mahajan et al. model presented in [6], both for stability of output to varying input parameters and for possible degeneracy. The Mahajan model has been chosen due to its currently being

P. Gemmell, B. Rodriguez and K. Burrage are with the Computing Laboratory, University of Oxford, Oxford, UK

K. Burrage is also with the Department of Mathematics, Queensland University of Technology, Brisbane, Australia

T. Alexander Quinn is with the Department of Physiology, Anatomy and Genetics, University of Oxford, Oxford, UK

Email: philip.gemmell@comlab.ox.ac.uk

the ‘state of the art’ rabbit model. If it can be shown that this model can display parameter degeneracy, it will have far-felt implications for the orthodoxy of accepting a parameter set as accurate based on phenomenological fitting. It is also hoped to demonstrate the stability of the model to small fluctuations, which can be considered usual for physiological cell-to-cell variation.

This is a preliminary investigation into the effects of parameter variation, and will examine changes in two ion currents:  $I_{CaL}$  and  $I_{Ks}$ ; more specifically, the peak conductances ( $g_{CaL}$  and  $g_{Ks}$ ) for these currents will be varied. These currents were chosen for variation due to their pronounced effect on the AP shape [7]. According to [7], [8],  $I_{CaL}$  is noted for its contribution to prolonging the depolarisation phase (the ‘plateau’ of the AP), whereas the importance of  $I_{Ks}$  is exhibited in the repolarisation of the cell. It is hoped the action of these two currents on the AP will allow investigation of a varied output landscape, giving suitable opportunity to investigate both stability and degeneracy in the model.

## II. METHODS

### A. Computational Set-Up

The Mahajan et al. model was downloaded from the CellML repository, and internal potassium concentration ( $[K^+]_i$ ) was unclamped. This new code was then converted by COR [9] to C++.

The Mahajan et al. model uses an extensive set of ODEs to model the cellular ionic currents, with a pseudo Markov model representing the  $I_{CaL}$  dynamics. A brief description of the formulation for  $I_{CaL}$  and  $I_{Ks}$  is given here; for further details of the model, the reader is referred to [6].

The  $I_{Ks}$  model equation is

$$I_{Ks} = g_{Ks} x_{s1} x_{s2} q_{Ks} (V_m - E_{Ks}), \quad (1)$$

where  $g_{Ks}$  represents the peak  $I_{Ks}$  conductance,  $x_{s1}$  and  $x_{s2}$  represent gating variables for the channel,  $q_{Ks}$  models the dependence of the channel on internal  $Ca^{2+}$ ,  $V_m$  is the membrane potential, and  $E_{Ks}$  represents the reversal potential for the channel. It should be noted that this formulation is based on the original equation set out in [1] with modifications found in [3], with further modifications to allow a fit with dynamic restitution data. The gating variables vary according to differential equations, with parameters that vary according to the value of  $V_m$ . The value of  $E_{Ks}$  depends on the internal

TABLE I  
VALUES OF CONSTANTS

| Parameter | Definition                 | Value                       |
|-----------|----------------------------|-----------------------------|
| $g_{Ca}$  | Peak $I_{CaL}$ conductance | 182 mmol $cm^{-1} C^{-1}$   |
| $g_{Ks}$  | Peak $I_{Ks}$ conductance  | 0.1386 mS $\mu F^{-1}$      |
| $F$       | Faraday's constant         | 93,485.339 C mol $^{-1}$    |
| $C_m$     | Cell capacitance           | $3.1 \times 10^4 \mu F$     |
| $v$       | Cell cytosol volume        | $2.58 \times 10^{-5} \mu l$ |

TABLE II  
RANGE OF PARAMETER VALUES USED

| Scale ( $g^{scale}$ ) | $g_{Ca}$<br>(mmol/cmC) | $g_{Ks}$<br>(mS/ $\mu F$ ) |
|-----------------------|------------------------|----------------------------|
| 0.1                   | 18.2                   | 0.01386                    |
| 0.5                   | 91.0                   | 0.06930                    |
| 0.6                   | 109.2                  | 0.08316                    |
| 0.7                   | 127.4                  | 0.09702                    |
| 0.75                  | 136.5                  | 0.10395                    |
| 0.8                   | 145.6                  | 0.11088                    |
| 0.9                   | 163.8                  | 0.12474                    |
| 1.0                   | 182.0                  | 0.13860                    |
| 1.1                   | 200.2                  | 0.15246                    |
| 1.2                   | 218.4                  | 0.16632                    |
| 1.25                  | 227.5                  | 0.17325                    |
| 1.3                   | 236.6                  | 0.18018                    |
| 1.4                   | 254.8                  | 0.19404                    |
| 1.5                   | 273.0                  | 0.20790                    |
| 2.5                   | 455.0                  | 0.34650                    |
| 5.0                   | 910.0                  | 0.69300                    |

and external concentrations of  $K^+$  and  $Na^+$ . All constant parameter values are given in Table I

Mahajan et al. models the L-type  $Ca^{2+}$  channel dynamics using a minimal seven-state Markovian model incorporating closed, open and inactive states for the channel. The resulting equations to describe  $I_{CaL}$  are given by

$$I_{Ca} = -2 \frac{Fv}{C_m} g_{Ca} P_o i_{Ca}, \quad (2)$$

where  $C_m$  is the membrane capacitance,  $v$  is the cytosol volume,  $g_{CaL}$  the strength of the  $Ca^{2+}$  current flux,  $P_o$  the probability the channels are open, and  $i_{Ca}$  is the unitary current through L-type  $Ca^{2+}$  channels (which changes with voltage).

Due to the non-compartmentalised, non-stochastic nature of the model, the effect of reducing ion channel conductances can be considered to either reduce the peak conductance of each individual ion channel, or to reduce the number of ion channels in the cell as a whole. Parameters are varied based on a scaling from their 'control' values—the consequent values are shown in Table II. This represents a broad-range sweep over the parameter space ([0.1, 5.0]), followed by a more in depth investigation of those scaling values closer to 1 ([0.5, 1.5]).

The model was solved using a forward Euler method with a time step of 0.005ms for a duration of 10 minutes. A stimulus current of  $12nA nF^{-1}$  was applied for 3ms to the model to generate a basic cycle length of 400ms—this is the same basic cycle length as was used in the original

formulation of the model in [6].

### B. Analysis of Results

The last two APs of the simulation are compared against each other with a least square difference method, both for membrane potential ( $V$ ) and internal calcium concentration ( $[Ca^{2+}]_i$ ), to ensure steady state has been reached. If the simulation is not at steady state, no further analysis is performed. If steady state is reached, the values for APD are calculated, for 90%, 50% and 30% repolarisation; APD is considered as the interval between  $dV/dt$  reaching its maximum value during the upstroke, and the membrane potential repolarizing to the specified percentage. Furthermore, the shape of the AP and the  $Ca^{2+}$  transient are compared to the control by summing the absolute difference between each recorded data value; data are recorded at intervals of 0.1ms. The calculation of both APD and absolute difference allows it to be established whether or not APD can be considered a reliable indicator of fit, or if the more rigorous (and more computationally intensive) absolute difference calculation is required to accurately assess goodness of fit.

## III. RESULTS AND DISCUSSION

Fig. 1 shows the results for APD, AP shape and  $Ca^{2+}$  transient shape differences from control to different parameter scaling values. They demonstrate that linear changes in the input parameter set do not lead to linear changes in the output—the precise structure of the output landscape is a complex matter, with the greatest differences in output not necessarily correlating to the greatest differences in input. This can be seen in fig. 1(F), which shows the similarity between the control AP and the AP produced when  $g_{CaL}$  and  $g_{Ks}$  are both scaled by five. It can be noted, however, that the plateau is noticeably shortened, implying  $I_{Ks}$  (which shortens the AP when increased) plays a greater role in AP shape determination than  $I_{CaL}$  (which lengthens the AP when increased). The results also indicate some robustness to small parameter variation, and furthermore that the impact on output by large variations in one parameter can be mitigated by large variations in another.

Fig. 2 shows the results for  $\pm 50\%$  parameter variation. It includes a plot of the control AP (Fig. 2(F)), and the AP for  $g_{Ca}^{scale} = 0.5, g_{Ks}^{scale} = 0.7$ . Comparison with Fig. 1(F) demonstrates that, in this instance, a smaller scaling of input parameters leads to a greater difference in the output—this is due mainly to the parameter set leading to a reduced 'plateau' potential, coupled with a more rapid repolarisation. The 'notch' of the AP does not appear to be greatly affected.

Steady state is not reached for the parameter set  $g_{Ca}^{scale} = 5.0, g_{Ks}^{scale} = \{0.5, 0.75, 0.9, 1.0, 1.1, 1.5\}$ —however, a stable form of alternans is reached (data not shown). Assuming increased  $I_{CaL}$  will lead to increased  $Ca^{2+}$  flux in the cell, this will in turn lead to increased interval  $Ca^{2+}$ . It is likely that this is the root cause for  $Ca^{2+}$  transient alternans, which in turn leads to  $V_m$  alternans, as opposed to  $V_m$  alternans causing  $Ca^{2+}$  alternans; further investigations will have to be conducted to verify this hypothesis in this instance. These

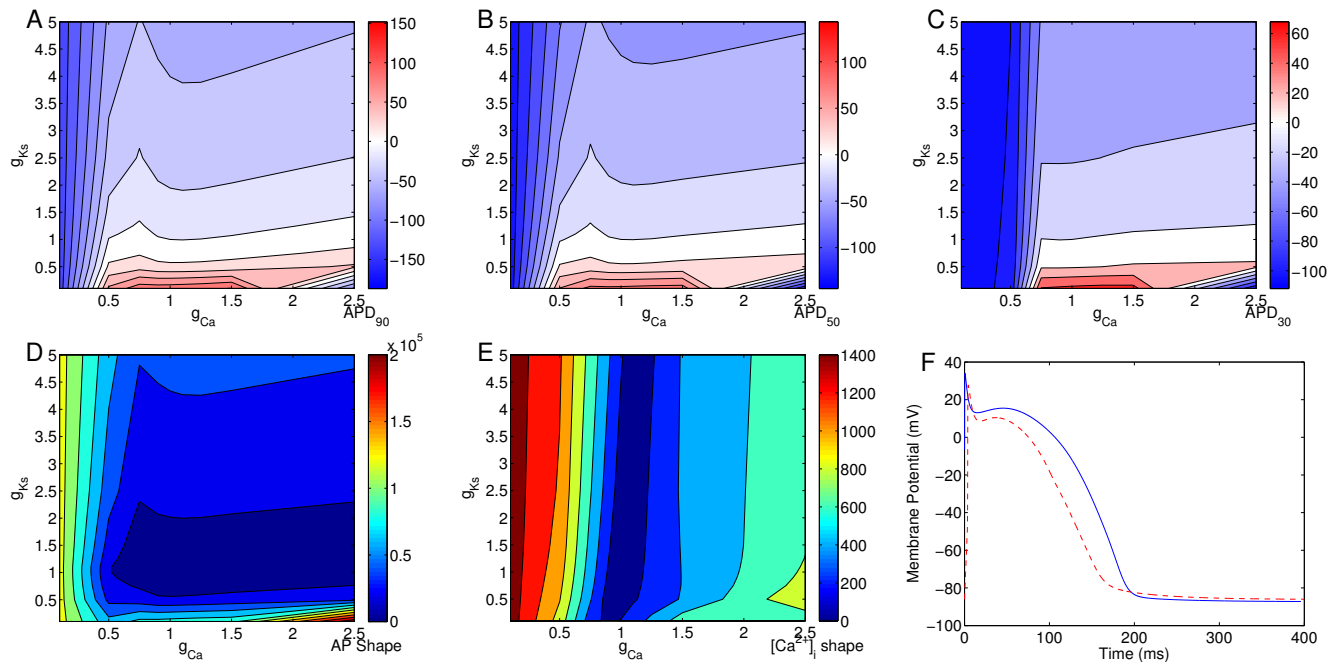


Fig. 1. Effects of varying  $g_{CaL}$  and  $g_{Ks}$ . (A)-(C) are contour plots displaying the difference between the control APD and the APD for the model with  $g_{CaL}$  and  $g_{Ks}$  scaled as indicated in the axes, for APD<sub>90</sub>, APD<sub>50</sub> and APD<sub>30</sub> respectively. (D) shows the summed absolute difference between control and simulation for the AP shape, and (E) the same for the  $Ca^{2+}$  transient. (F) plots the AP for the control input parameter values (solid line) and for the scaling by 5.0 (dashed line). Since steady state was not reached for some simulations with  $g_{Ca}^{scale} = 5$ , results for  $g_{Ca}^{scale} = 5$  have been excluded from the contour plots—the next available data for  $g_{CaL}$  are  $g_{Ca}^{scale} = 2.5$ .

results, combined with the result of scaling both  $g_{CaL}$  and  $g_{Ks}$  to five times their control value, imply an increased  $Ca^{2+}$  transient with no off-setting mechanism in place (e.g. increased  $I_{Ks}$ ) has a profound impact on the AP.

It is worth noting that  $g_{Ca}^{scale} = 5.0$ ,  $g_{Ks}^{scale} = 1.25$  produced a steady state output (data not shown)—this ‘island’ of stability in the range noted above serves to emphasise the non-linear, non-trivial nature of the interactions between currents.

The results also show significant differences between the results for APD difference and for the AP shape absolute difference. All APD data demonstrated similar results, but the contour plot for AP shape is markedly different. These results suggest that APD is not sufficient to fully assess the similarity between two different AP traces. It is also worth noting the different landscape for AP shape and  $Ca^{2+}$  transient shape, demonstrating their different reactions to input parameter variation. This indicates that a model may provide a very good fit by one metric, and yet may be entirely inaccurate when measured against a different metric.

Comparing the landscapes for all five contour plots, it is by no means certain that degeneracy for input parameter values exist—the results suggest a ‘trough’ in the landscape for APD, thus suggesting a degeneracy, but this trough does not appear to coincide with another trough for AP and  $Ca^{2+}$  shape, and thus, for the parameter set examined, the model does not exhibit degeneracy.

## IV. CONCLUSION AND FURTHER WORK

### A. Conclusions

This paper has succeeded in demonstrating the stability of the Mahajan model to small variations in input parameters. Furthermore, the AP appears to be stable to large variations in  $g_{CaL}$  and  $g_{Ks}$  if both are scaled by a similar amount. It has also been shown that the interaction between currents leads to non-linear, non-trivial changes in the output given differing inputs, and full simulation is required to demonstrate the output—prediction based on input parameters is not always possible. The results also indicate that APD is insufficient on its own as an indicator of goodness of fit for AP output, and that the ‘success’ of a model can be judged by many different metrics. The fact that different metrics may provide different answers for the accuracy of a model indicates a phenomenological fitting approach may not always be appropriate.

### B. Further Work

The work presented in this study is preliminary: it examines the effects of changing only two parameters for ionic channel conductance. Further work will extend this—using the Nimrod/G grid computing system [10], it is hoped to be able to conduct a parameter sweep over a  $\pm 30\%$  range for four other ion channel conductances ( $g_{Kr}$ ,  $g_{kl}$ ,  $g_{NaK}$ ,  $g_{to}$ ) in addition to  $g_{Ca}$  and  $g_{Ks}$ . Investigation of this six-dimensional parameter space will hopefully provide greater insights into the possibility of parameter degeneracy in model output, and indicate future directions for experimental investigations of

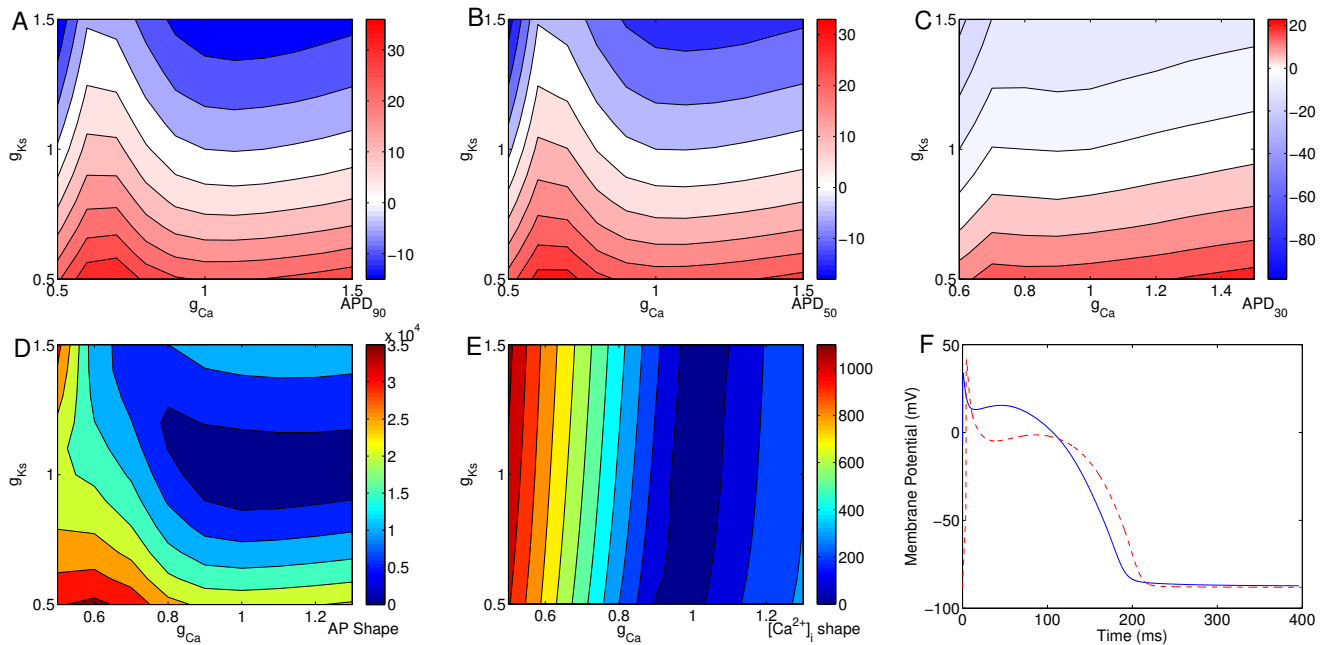


Fig. 2. Effects of varying  $g_{CaL}$  and  $g_{Ks}$  near the control value. (A)-(C) are contour plots displaying the difference between the control APD and the APD for the model with  $g_{CaL}$  and  $g_{Ks}$  scaled as indicated in the axes, for  $APD_{90}$ ,  $APD_{50}$  and  $APD_{30}$  respectively. (D) shows the summed absolute difference between control and simulation for the AP shape, and (E) the same for the  $Ca^{2+}$  transient. The parameter range shown in (C) is smaller than in the other plots—the reason for this is demonstrated in (F), which plots the AP for the control input parameter values (solid line) and for  $g_{CaL}^{scale} = 0.5$ ,  $g_{Ks}^{scale} = 0.7$ . The rapid initial repolarisation leads to values for  $APD_{30}$  that are far smaller than for any other simulation result. Consequently, the contour levels in (C) would be dominated by displaying those values.

parameter values. Work will also be conducted to adapt the Mahajan model from its current cellular regime to tissue by including terms to account for inter-cellular coupling. This will allow the predictions of the model to be compared to experimental data from rabbit ventricular tissue, and thus the accuracy of the model to empirical data can be assessed.

## V. ACKNOWLEDGMENTS

P.G. is funded by the EPSRC through the Systems Biology DTC. B.R. holds a UK MRC Career Development Award. T.A.Q. holds a UK EPSRC Postdoctoral Fellowship.

## REFERENCES

- [1] C.H. Luo and Y. Rudy, A Dynamic Model of the Cardiac Ventricular Action Potential I, *Circ. Res.*, vol. 74, 1994, pp 1071-1096.
- [2] J.L. Puglisi and D.M. Bers, LabHEART: an interactive computer model of rabbit ventricular myocyte ion channels and Ca transport, *Am. J. Physiol. Cell Physiol.*, vol. 281, 2001, pp C2049-C2060.
- [3] T.R. Shannon, F. Wang, J. Puglisi, C. Weber and D.M. Bers, A Mathematical Treatment of Integrated Ca Dynamics within the Ventricular Myocyte, *Biophys. J.*, vol. 87, 2004, pp 3351-3371.
- [4] J. G. Restrepo, J. N. Weiss and A. Karma, Calsequestrin-Mediated Mechanism for Cellular Calcium Transient Alternans, *Biophys. J.*, vol. 95, 2008, pp 3767-3789.
- [5] W. Chen, J. A. Wasserstrom and Y. Sherifaw, Role of coupled gating between cardiac ryanodine receptors in the genesis of triggered arrhythmias, *Am. J. Physiol. Heart Circ. Physiol.*, vol. 297, 2009, pp H171-H180.
- [6] A. Mahajan, Y. Sherifaw, D. Sato, A. Baher, R. Olcese, L.H. Xie, M.J. Yang, P.S. Chen, J.G. Restrepo, A. Karma, A. Garfinkel, Z. Qu and J.N. Weiss, A Rabbit Action Potential Model Replicating Cardiac Dynamics at Rapid Heart Rates, *Biophys. J.*, vol. 94, 2008, pp 392-410.
- [7] E. Carmeliet and J. Vereecke, *Cardiac Cellular Electrophysiology*, Kluwer Academic Publishers; 2002.
- [8] D. M. Roden, J. R. Balsler, A. L. George Jr. and M. E. Anderson, Cardiac Ion Channels, *Annu. Rev. Physiol.*, vol. 64, 2002, pp 431-475.
- [9] A. Garny, P. Kohl and D. Noble, Cellular Open Resource(COR): a public CellML based environment for modelling biological function, *Int. J. Bif. Chaos*, vol. 13, 2003, pp 3579-3590.
- [10] D. Abramson, J. Giddy and L. Kotler, High Performance Parametric Modeling with Nimrod/G: Killer Application for the Global Grid?, *International Parallel and Distributed Processing Symposium (IPDPS)*, Cancun, Mexico, May 2000, pp 520-528.